

A composite H II region luminosity function in H α of unprecedented statistical weight

T. R. Bradley^{1,2}, J. H. Knapen², J. E. Beckman^{3,4}, and S. L. Folkes²

¹ Centre for Astrophysics, University of Central Lancashire, Preston PR1 2HE, UK

² Centre for Astrophysics Research, University of Hertfordshire, Hatfield, Herts AL10 9AB, UK
e-mail: j.knapen@star.herts.ac.uk

³ Instituto de Astrofísica de Canarias, E-38200 La Laguna, Spain

⁴ Consejo Superior de Investigaciones Científicas, Spain

Received ; accepted 15 Sep. 2006

ABSTRACT

Context. Statistical properties of H II region populations in disk galaxies yield important clues to the physics of massive star formation. *Aims.* We present a set of H II region catalogues and luminosity functions for a sample of 56 spiral galaxies in order to derive the most general form of their luminosity function.

Methods. H II region luminosity functions are derived for individual galaxies which, after photometric calibration, are summed to form a total luminosity function comprising 17,797 H II regions from 53 galaxies.

Results. The total luminosity function, above its lower limit of completeness, is clearly best fitted by a double power law with a significantly steeper slope for the high luminosity portion of the function. This change of slope has been reported in the literature for individual galaxies, and occurs at a luminosity of $\log L = 38.6 \pm 0.1$ (L in erg s^{-1}) which has been termed the Strömgren luminosity. A steep fall off in the luminosity function above $\log L = 40$ is also noted, and is related to an upper limit to the luminosities of underlying massive stellar clusters. Detailed data are presented for the individual sample galaxies.

Conclusions. The luminosity functions of H II regions in spiral galaxies show a two slope power law behaviour, with a significantly steeper slope for the high luminosity branch. This can be modelled by assuming that the high luminosity regions are density bounded, though the scenario is complicated by the inhomogeneity of the ionized interstellar medium. The break, irrespective of its origin, is of potential use as a distance indicator for disc galaxies.

Key words. galaxies: spiral – galaxies: structure – ISM: H II regions

1. Introduction

In their paper giving a major overview of the luminosity functions (LFs) in H α emission of the H II regions in disk galaxies Kennicutt, Edgar & Hodge (1989; hereafter KEH) noted that an important subset of their objects showed LFs with a clear break in slope at a luminosity of $L(\text{H}\alpha) = 38.7$ dex (units of erg s^{-1}). At lower luminosities the power law slope is flatter, whereas above the break it is steeper. KEH called those LFs showing a break “type II”, suggesting that any galaxy will exhibit type II behaviour if it has sufficient high luminosity H II regions. A galaxy with sufficient luminous H II regions to show a clear break, M51, was observed by Rand (1992), who measured it at $L(\text{H}\alpha) = 38.6$ dex. Rand’s work, using CCD data, was especially precise, and revealed, as well as the break, a narrow peak in the LF close to the break luminosity. In the LF of M33, Hodge et al. (1999) found no break, which is not surprising since the function is defined only up to $L(\text{H}\alpha) = 38.4$ dex, with only a dozen regions above $L(\text{H}\alpha) = 38$ dex. Further examples of this type are NGC 6822 and the dwarf galaxy Holmberg II (Hodge, Strobel & Kennicutt 1994), smaller galaxies with small H II region numbers at $L(\text{H}\alpha) > 38$ dex. On the other hand, M101 has some 60 H II regions with $L(\text{H}\alpha) > 38.5$ dex and shows a clear break at $L(\text{H}\alpha) 38.6$ dex (Scowen, Dufour & Hester 1992). Our group has published LFs for galaxies selected to have large num-

bers of high luminosity H II regions to test the suggestion that the break luminosity shows low scatter. In three articles (Rozas, Beckman & Knapen 1996; Rozas et al. 1999; and Rozas, Zurita & Beckman 2000), eight galaxies were measured and all showed type II LFs, most strikingly NGC 7479, which has the largest number of luminous H II regions.

In spite of the general result reported in KEH, and in spite of the type II LFs found in individual objects, the question has been raised persistently whether the break is a real feature or an artifact. Two types of doubts can be found in the literature. One claims that although breaks can be found, they are not a universal physical feature, as the break luminosity varies over quite a wide range between objects. One example here is by Thilker, Braun & Walterbos (2000) who derived an LF for M51 using an automated method, finding a break at 38.9 dex, compared with the value of 38.6 by Rand (1992) who used an interactive, region by region method. The point raised is whether for statistical reasons connected with the chosen binning parameters a clear break luminosity cannot be derived, given the low number of regions per luminosity bin. Others have not found consistent evidence for breaks, and certainly not at a specific luminosity, among these being González Delgado & Pérez (1997) in an H α survey of 27 galaxies selected for their nuclear activity. Their sample comprised some 2000 H II regions, i.e., ≈ 75 per galaxy in a luminosity range from $L(\text{H}\alpha) = 37$ dex to 39.5 dex. The numbers per bin above 38.5 dex are on average quite small for each galaxy which would lead to difficulty in detecting breaks.

On completing a recent imaging survey in H α of a set of nearby galaxies (Knapen et al. 2004) we saw that we could make a significant test of the suggestion that a dual slope LF with a well defined break gives a better general description than a single power law slope, and that the original result of KEH, with its clean break at a specific luminosity, is present in a data set with a sufficient statistical base. Our observations have allowed us to isolate and catalogue almost 18,000 H II regions in 56 galaxies. Here we give the key results of this study and also offer on-line catalogues for the full set of objects.

2. Sample selection and H α imaging

2.1. Sample selection and observations

We have used the data set published by Knapen et al. (2004), which contains a full set of continuum-subtracted H α images of 57 relatively face-on ($i < 50^\circ$), nearby, Northern, spiral galaxies. Most of the images were obtained with the 1 m Jacobus Kapteyn Telescope (JKT), but some with other telescopes or from the literature. Most of the H α images were taken through $\approx 50\text{\AA}$ wide filters matched to the recessional velocity of each galaxy. Full details on the observations are given in Knapen et al. (2004), whereas the sample galaxies are listed, and their distances, plate scales, and resolutions given, in Table 1 (**online only**).

2.2. The effects of seeing on H II region selection

The FWHM seeing in our H α images varies from 0.8 to 3.7 arcsec (1.53 arcsec in the median), which corresponds to a range in spatial resolution of 30 to 295 pc (137 pc in the median). We thus need to consider possible effects of blending on the resulting H II region catalogues. The two major effects are that fainter H II regions may be spatially coincident with larger, brighter, H II regions, reducing the number of faint H II regions observed, and overlapping of H II regions, which may lead to a measured luminosity higher than the true luminosity. KEH showed that whereas degrading images up to resolutions of 200 pc had little effect on the luminosities of interest here, and that degrading them to a resolution of 200-400 pc will affect the faint end of the luminosity function while preserving the shape of the upper LF, blending seriously affects the entire LF and causes increases in the luminosities of first ranked H II regions in images with a resolution of 300-500 pc. Rand (1992) modelled the main effects of blending for the arm LF of M51, and found that they did not significantly affect the shape of the LF.

More recently, H α LFs have been derived from *HST* imaging (Pleuss, Heller & Fricke 2000; Scoville et al. 2001), which has significantly higher spatial resolution than the typical size of an H II region in the luminosity range of interest here. Under these circumstances, it is possible to classify a single H II region, due to a single coeval OB association, artificially as a set of aggregated H II regions, each of a lower luminosity.

We thus conclude that blending should not have serious consequences for the main results presented in this letter, although for individual galaxies at larger distances blending may introduce uncertainties in the LFs.

3. Calibration

The continuum subtraction and photometric calibration of the H α images has been described in detail by Knapen et al. (2004). We estimated the uncertainties in the calibration to be $L =$

0.1 dex by assuming errors of 3% in the distance to the galaxy, and of one standard deviation of the adopted background value of the calibration star.

Since the final continuum-subtracted images of most galaxies contain emission from both the H α line and the [N II] lines at 6548 \AA and 6583 \AA , we need to correct for the latter before determining the star formation rates. We do this by assuming a fixed ratio between the [N II] 6583 and 6548 lines of three, and a value η for the [N II] 6583/H α ratio of 0.25 for galaxies that do not contain any or only a few ‘‘giant’’ H II regions (e.g., early-type galaxies) and of 0.16 for the later Hubble types, based on descriptions in Osterbrock (1989). We compute the final correction factor for each galaxy by additionally determining the relative filter transmissions in the H α and [N II] lines, for which we used the filter transmission characteristics as measured by the Isaac Newton Group (ING), which operated the JKT.

We found that the [N II] contribution varied due to filters used, recessional velocity, and galaxy type, and ranged from 9% to 36% with a mean of 17%. NGC 3631 and NGC 4321 were both observed with H α filters of width 15 \AA which was narrow enough not to include any [N II] emission.

Thilker et al. (2002) use values of η which vary from 0.1 to 0.4, but only one galaxy is common to both their and our sample. This is NGC 5457, for which Thilker et al.’s value is 0.2, as opposed to ours of 0.16. Using the former value would lead to a difference of 3% in the [N II] contribution to our image, which is not a significant factor in the analysis of the LF. No other such comparisons could be made from the literature.

4. H II region catalogues

We used a semi-automatic method to derive the H II region catalogues for all sample galaxies which uses the REGION programme (C. H. Heller, private communication; see Rozas et al. 1999; Pleuss et al. 2000). Using a tree algorithm, REGION catalogues each H II region, yielding the position of its centre, its area in pixels and its background-subtracted flux. An advantage of REGION over any fully automated programme is that it allows for defining local backgrounds, and for manual editing of the resulting catalogue to remove features like cosmic rays or remnants of imperfect continuum subtraction of foreground stars. We chose not to catalogue H II regions in the central 1 kpc region of each galaxy for two reasons. Firstly, crowding and blending is especially severe there, and secondly, especially in the AGN hosts in our sample, the H α can be severely contaminated by emission resulting from shocks or AGN emission. The H II region catalogues are all available electronically through the Centre de Données Stellaires (CDS)¹. The catalogues list for all galaxies a number identifying the H II region (col. 1), the position of the pixel of maximum intensity of the H II region relative to the centre of the galaxy, in RA and dec (pixel scale is 0.241 arcsec pixel⁻¹; cols. 2 and 3), the logarithm of its integrated luminosity in erg s⁻¹ (col. 4), the area of the H II region in units of pc² (col. 5), and the value of the local background (col. 6).

5. Luminosity functions

5.1. Individual galaxies

On the basis of our H II region catalogues, we constructed luminosity functions (LFs) for all our galaxies, which we present in

¹ Via anonymous ftp to cdsarc.u-strasbg.fr (130.79.128.5) or via <http://cdsweb.u-strasbg.fr/cgi-bin/qcat?J/A+A/>

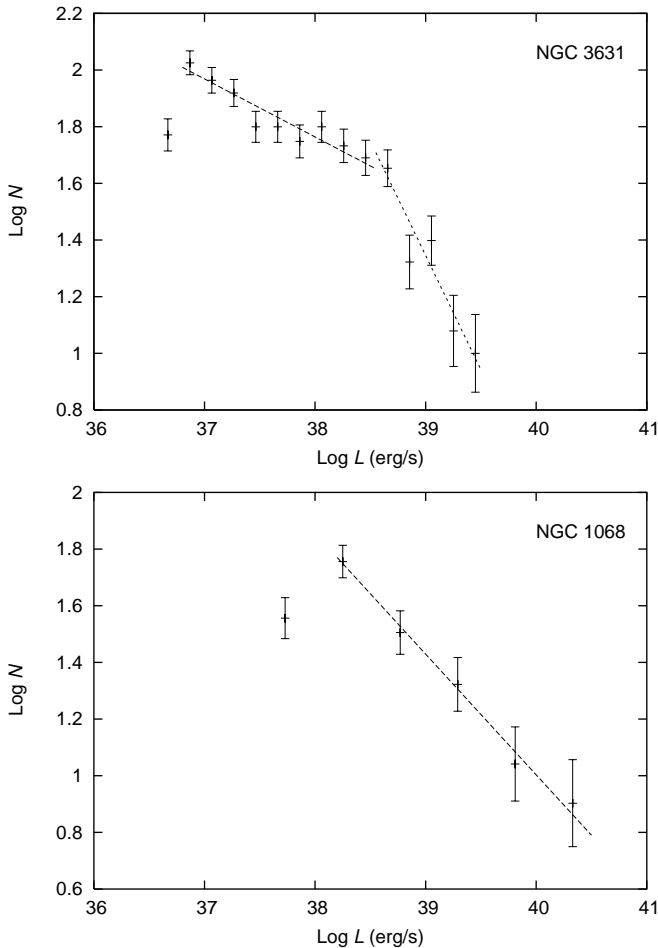


Fig. 2. H II region LFs of NGC 3631 (*top panel*), whose catalogue contains 801 H II regions, fitted with a double power law, and of NGC 1068 (*lower panel*), with 166 H II regions, and fitted with a single power law. The LFs have been plotted with bin widths of 0.2 and 0.5 dex, respectively.

Fig. 1 (**online only**). The bin widths for plotting and fitting were determined following Scott (1979), and vary from 0.2 to 0.7 dex as a function of the number of H II regions (see Table 1). We fit slopes to the LFs, following the equation $N(L)dL = AL^{-a}dL$, where $N(L)dL$ is the number of H II regions with luminosities in the range L to $L + dL$, and a is the slope, as introduced by KEH. Consistent with KEH and most of the more recent work, we made an adjustment of -1 to the slopes of the plotted LFs, which is due to the fact that we show differential LFs as determined with logarithmic binning, whereas the slopes refer to a differential LF with linear binning. The slopes, as determined with a weighted fit, have been plotted on the LFs in Fig. 1, and are listed, along with their formal errors and coefficients of determination r^2 , in Table 1.

KEH pointed out (see also, e.g., Rand 1992; Beckman et al. 2000) that for those galaxies which have large enough numbers of H II regions with $L > 39$ dex, the LFs were, in general, best fitted with a double power law, with the fit to the higher- L portion of the LF steeper-sloped than that of the lower- L portion. This is borne out in the present sample, where only eight of our galaxies satisfy the requirement of sufficient high- L H II regions to entail a statistically significant double power law fit. Fitting the LFs of these galaxies with a single power law gives a demonstrably inferior fit. Parameters of the single power law fits are listed in

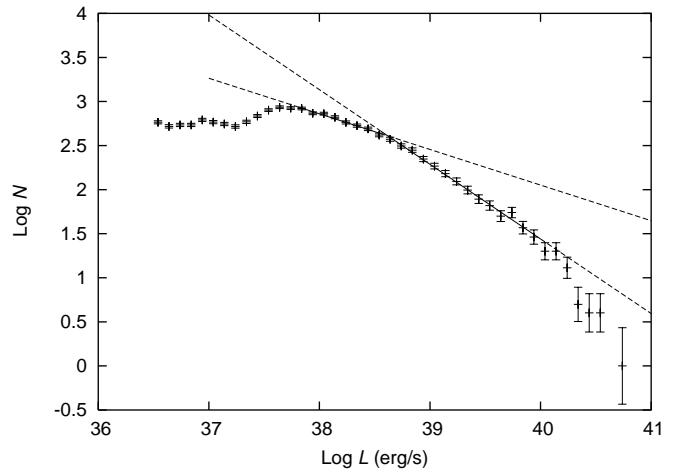


Fig. 3. LF made from the combined H II region catalogues of 53 of our sample galaxies. The large number of H II regions allows plotting the LF in steps of 0.1 dex. The best double-slope fit is indicated by the lines, where dashes show extrapolations beyond the range over which the best fit has been made.

Table 1 for all those galaxies in the sample with sufficient H II regions to do this reliably, whereas the results of the double fits are listed in Table 2 (**online only**). Fig. 2 shows representative examples of a galaxy where a double fit is superior (*top panel*) and of one with insufficient high- L H II regions (*lower panel*).

5.2. Composite luminosity functions

In the present *Letter*, our purpose is to discuss the combined LF for the complete sample (rather than to use separately the individual LFs shown in Fig. 1). We can produce a combined LF because all our data have been uniformly calibrated photometrically, and because, separating the sample into three basic morphological blocks: early, intermediate and late types, we did not find significant differences in the slopes of the low or high luminosity portions of the LF. The result, which contains 17,797 H II regions, is shown in Fig. 3 (bin width 0.1 dex). Overlaid on that Figure is the best double power law fit ($a_{\text{upper}} = -1.36 \pm 0.02$, $r^2 = 0.98$; $a_{\text{lower}} = -1.86 \pm 0.03$, $r^2 = 1.00$). A single power law can be fitted ($a_{\text{single}} = -1.58 \pm 0.01$, $r^2 = 0.94$), but has a significantly lower coefficient of determination. The low- L limit to the fitted range occurs at a value of $L = 37.6$ dex, which is a completeness limit imposed by a combination of signal-to-noise ratio and spatial resolution in the H α images. As we will see below, this completeness limit occurs well below the break luminosity and allows fits to both the low and high- L slopes.

Not only does the statistical strength of our combined LF of almost 18,000 H II regions allow us to confirm so clearly *that* a break occurs in the LF slope, but the quality of our data is good enough for us to establish exactly *where* that break occurs. We made successive fits to the two slopes, varying the break luminosity between $L = 37.7$ dex and 39.1 dex. Fig. 4 shows the parameter which best indicates the quality of each fit, the coefficient of determination, r^2 , as a function of log L for both the lower and upper slopes. Before interpreting the results, we must note that r^2 will move closer to unity (indicating better fits) as more points are fitted, which will occur for higher break- L for the lower- L slope, and vice versa for the upper slope. Even so, Fig. 4 clearly shows a maximum for each slope, indicating a distinct and restricted range of log L where the best fit quality is

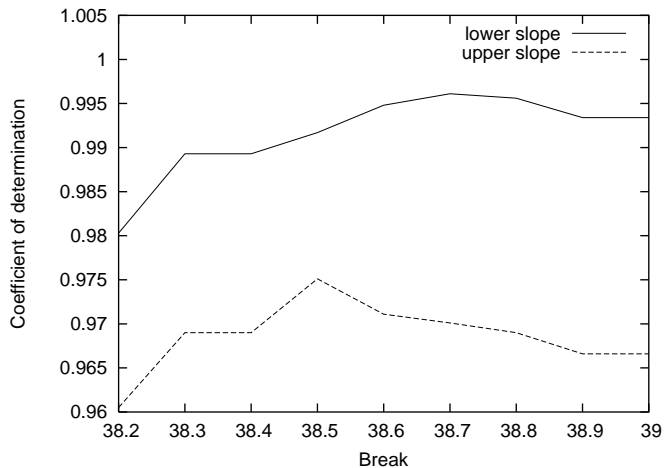


Fig. 4. Coefficient of determination, r^2 , for the upper and lower slopes of the double-slope fit to the combined LF of Fig. 3, as a function of the $\log L$ at which the break between the two slopes occurs. Better fits are closer to $r^2 = 1$, so the best fit is achieved for a break at $\log L(\text{erg s}^{-1}) = 38.6 \pm 0.1$, the average of the best values for the low and high- L slopes.

obtained. The resulting value for the break, or Strömgren, luminosity is $\log L(\text{erg s}^{-1}) = 38.6 \pm 0.1$.

Theoretical explanations for the break have been discussed previously, notably by Beckman et al. (2000) who suggested that it might be caused by the transition from ionisation bounding to density bounding as the H II regions become more luminous, and who made semi-quantitative predictions of the relations between the slopes of the two power laws based on this scenario. Pleuss et al. (2000) argued that the effect might be due to a clustering property in which H II regions of increasing luminosity have an increasing probability of absorbing smaller H II regions by overlap, and that this may be subject to a scaling law related to the separation between star formation regions. Any quantitative attempt to implement the latter or similar proposals, however, leads to an LF in which the upper luminosity slope is shallower, not steeper, than that in the lower luminosity range. So the density bounding scenario retains its basic plausibility, although it must be carefully quantified to take into account the fact that H II regions are highly clumpy (see, e.g., Giammanco et al. 2004 for a study of how clumpiness affects the propagation of ionising radiation in H II regions), rather than being idealised Strömgren spheres of uniform density. An alternative explanation is the one proposed by Oey & Clarke (1998), in which the break in the LF is due to the evolution of the H α luminosities of the H II regions.

It is interesting to note that at the high luminosity end of the LF, above $L = 40$ dex, the curve falls away quite sharply. It is true that the number of H II regions per bin in this range is small, and this is shown clearly in Fig. 3 in the increasing amplitude of the error bars as L increases. The LF would take this form if we were seeing a true cut-off in the luminosity of H II regions due to a physical limit on the masses of high mass stars modulated by a statistical effect due to the variation of the total stellar mass in young clusters. Before reaching a firm conclusion on this, however, it would be useful to be able to increase the statistical base in this range by further observations.

6. Summary and concluding remarks

We have analysed continuum-subtracted H α images of 57 nearby galaxies, and here present the LFs and catalogues of their populations of H II regions. Using the combined data set we have produced a single LF covering the range in H α luminosity from $L = 37.5$ dex to just over $L = 40$ dex. The total number of H II regions contributing to this LF is a little under 18,000, which is almost an order of magnitude greater than that of any previously published LF of this type. The best functional fit of the LF, above the completeness limit, is by a double power law, having a break at $L = 38.6$ dex, with the steeper slope to higher luminosity and the shallower slope to lower luminosity. The existence of this break suggests a change in physical regime going from lower to higher H α luminosity. If confirmed, and by virtue of its occurrence at high H II region luminosities, the break is of potential use as a distance indicator for star-forming disk galaxies.

The number of H II regions in our sample is large enough to suggest that the steep fall off in the LF above $L = 40$ dex indicates that we are sampling the range where there is a cut-off in the luminosities of the H II regions, implying a drop-off in the LF of the underlying massive stellar clusters. This is giving us potentially important information about a physical limit to the masses of stars in young clusters of varying total stellar mass.

Acknowledgements. We thank the anonymous referee for a number of excellent suggestions which helped improve this Letter. J.H.K. acknowledges support of the Leverhulme Trust in the form of a Leverhulme Research Fellowship, while S.L.F. thanks the Royal Astronomical Society for the award of a summer student bursary. This research was partly supported by Project AYA-2004-08251-CO2-01 of the Spanish Ministry for Education and Science, and by Project P3/86 of the Instituto de Astrofísica de Canarias. The JKT has been operated on the island of La Palma by the ING in the Spanish Observatorio del Roque de los Muchachos of the Instituto de Astrofísica de Canarias. This research has made use of the NASA/IPAC Extragalactic Database (NED) which is operated by the Jet Propulsion Laboratory, California Institute of Technology, under contract with the National Aeronautics and Space Administration.

References

- Giammanco, C., Beckman, J. E., Zurita, A., & Relaño, M. 2004, A&A, 424, 877
- González Delgado, R. M., & Pérez, E. 1997, ApJS, 108, 199
- Hodge, P. W., Balsley, J., Wyder, T. K., & Skelton, B. P. 1999, PASP, 111, 685
- Hodge, P., Strobel, N. V., & Kennicutt, R. C. 1994, PASP, 106, 309
- Kennicutt, R. C., Jr., Edgar, B. K., & Hodge, P. W. 1989, ApJ, 337, 761 (KEH)
- Knapen, J. H., Stedman, S., Bramich, D. M., Folkes, S. L., & Bradley, T. R. 2004, A&A, 426, 1135
- Oey, M. S., & Clarke, C. J. 1998, AJ, 115, 1543
- Pleuss, P. O., Heller, C. H., & Fricke, K. J. 2000, A&A, 361, 913
- Rand, R. J. 1992, AJ, 103, 815
- Rozas, M., Beckman, J. E., & Knapen, J. H. 1996, A&A, 307, 735
- Rozas, M., Zurita, A., & Beckman, J. E. 2000, A&A, 354, 823
- Rozas, M., Zurita, A., Heller, C. H., & Beckman, J. E. 1999, A&AS, 135, 145
- Scott, D. W. 1979, Biometrika, 66, 605
- Scoville, N. Z., Polletta, M., Ewald, S., Stolovy, S. R., Thompson, R., & Rieke, M. 2001, AJ, 122, 3017
- Scowen, P. A., Dufour, R. J., & Hester, J. J. 1992, AJ, 104, 92 (Erratum 1994, AJ 107, 1203)
- Thilker, D. A., Braun, R., & Walterbos, R. A. M. 2000, AJ, 120, 3070

Online Material

NGC	Type	Upper Slope	Lower Slope	Break log L
628	Sc	-1.26 ± 0.03	-2.05 ± 0.10	N/A
3184	Sc	-1.35 ± 0.10	-2.14 ± 0.11	38.7 ± 0.1
3631	Sbc	-1.21 ± 0.03	-1.81 ± 0.16	38.6 ± 0.1
4123	SBbc	-1.32 ± 0.09	-2.32 ± 0.28	38.7 ± 0.1
4151	Sab	-1.17 ± 0.09	-2.10 ± 0.22	38.3 ± 0.1
4254	Sc	-1.22 ± 0.08	-2.12 ± 0.13	38.7 ± 0.1
4321	Sc	-1.72 ± 0.10	-1.97 ± 0.41	38.6 ± 0.1
6946	Sc	-1.44 ± 0.03	-2.81 ± 0.27	38.2 ± 0.1

Table 2. (Online only) Double fits to LFs for those galaxies whose LFs allowed such fits.

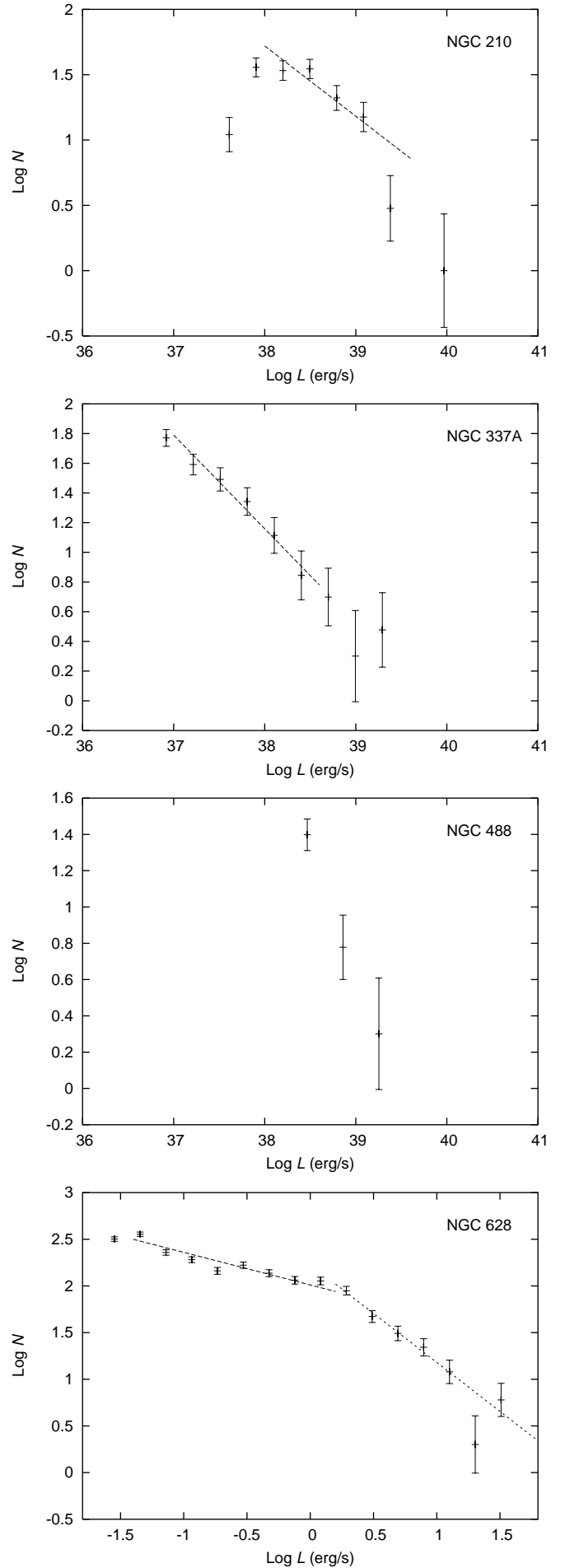


Fig. 1. Online only LFs of 56 of our sample galaxies, with best

NGC	Cal. log(L)	Compl. log(L)	N	Scale (pc/'')	D (Mpc)	Res. (pc)	max log(L)	min log(L)	bin width (dex)	slope	error	r^2
210	38.49	38.40	396	98	20.3	151	39.95	37.64	0.3	-1.54	0.13	0.725
337A	37.94	37.07	189	66	13.7	94	39.44	36.78	0.3	-1.63	0.07	0.965
488	38.46	38.37	35	142	29.3	209	39.45	38.28	0.4	Too few H II regions		
628	N/A	N/A	2027	47	9.7	54	No photometric data		0.2	-1.25	0.03	0.899
864	38.35	38.15	227	97	20	133	40.32	37.84	0.3	-1.40	0.09	0.726
1042	38.21	37.65	158	81	16.7	133	39.35	37.36	0.3	-1.57	0.09	0.985
1068	38.41	38.16	166	70	14.4	157	40.59	37.48	0.5	-1.43	0.06	0.994
1073	38.08	37.41	170	74	15.2	100	39.37	37.10	0.5	-1.49	0.07	0.970
1169	36.65	PQ	26	163	33.7	295	36.52	35.74	0.4	Too few H II regions		
1179	37.47	PQ	18	103	21.2	228	38.46	37.11	0.5	Too few H II regions		
1300	38.42	38.03	84	91	18.8	206	39.60	37.93	0.3	-1.68	0.16	0.883
2775	38.17	37.53	66	82	17	156	38.70	37.44	0.3	Too few H II regions		
2805	38.23	38.02	94	136	28	229	39.76	37.65	0.4	-1.47	0.14	0.924
2985	38.37	37.92	338	109	22.4	194	39.16	37.40	0.2	-1.54	0.09	0.931
3184	37.85	37.92	576	42	8.7	73	39.25	36.63	0.2	-1.35	0.10	0.733
3227	38.71	37.34	190	100	20.6	142	39.39	37.05	0.4	Too few H II regions		
3344	37.22	36.66	669	30	6.1	41	38.56	36.38	0.2	-1.52	0.05	0.920
3351	37.53	37.42	55	39	8.1	62	38.66	37.33	0.6	Too few H II regions		
3368	37.44	36.98	77	39	8.1	68	38.68	36.89	0.3	-1.72	0.18	0.945
3486	37.27	36.55	612	36	7.4	46	38.83	36.30	0.2	-1.43	0.04	0.895
3631	33.88	36.87	801	105	21.6	137	39.54	36.57	0.2	-1.21	0.03	0.896
3726	38.28	37.17	614	82	17	115	39.48	36.82	0.2	-1.45	0.05	0.915
3810	37.19	36.23	400	82	16.9	107	38.66	35.96	0.3	-1.14	0.04	0.725
4030	38.89	38.03	276	126	25.9	194	39.96	37.74	0.2	-1.08	0.07	0.107
4051	38.12	37.60	232	82	17	124	39.49	37.28	0.3	-1.28	0.10	0.933
4123	38.88	37.56	250	123	25.3	166	39.89	37.47	0.3	-1.40	0.06	0.941
4145	N/A	PQ	35	100	20.7	270	No photometric data		0.4	Too few H II regions		
4151	38.69	36.00	263	98	20.3	146	39.48	36.98	0.3	-1.17	0.086	0.972
4242	N/A	PQ	44	36	7.5	114	No photometric data		0.4	Too few H II regions		
4254	38.09	37.80	626	81	16.8	123	39.92	37.51	0.2	-1.22	0.08	0.833
4303	38.13	37.81	873	74	15.2	105	40.10	37.32	0.2	-1.44	0.04	0.952
4314	37.93	NDR	14	47	9.7	84	No photometric data		No disk regions			
4321	34.26	37.20	2647	81	16.8	80	40.15	36.93	0.2	-1.72	0.10	0.957
4395	35.78	35.90	498	18	3.6	32	38.66	35.60	0.3	-1.52	0.05	0.979
4450	N/A	PQ	32	81	16.8	70	No photometric data		0.6	Too few H II regions		
4487	38.38	37.64	146	97	19.9	192	39.84	37.46	0.3	Too few H II regions		
4535	38.20	7.64	518	81	16.8	152	39.82	37.34	0.2	-1.51	0.05	0.924
4548	38.12	37.48	74	81	16.8	141	38.90	37.20	0.3	-1.83	0.16	0.961
4579	38.04	37.38	121	81	16.8	127	39.75	37.07	0.4	-1.60	0.15	0.973
4618	37.67	36.44	290	35	7.3	46	38.89	36.15	0.4	Too few H II regions		
4689	38.26	37.50	160	81	16.8	146	39.20	37.17	0.3	-1.40	0.14	0.786
4725	37.97	37.82	134	60	12.4	140	39.51	37.32	0.3	-1.90	0.11	0.969
4736	36.91	36.39	294	21	4.3	30	37.82	36.09	0.4	-1.55	0.13	0.972
5247	38.79	38.23	157	108	22.2	247	40.27	38.14	0.3	-1.20	0.13	0.525
5248	38.48	37.72	381	110	22.7	156	40.18	37.63	0.3	-1.42	0.04	0.945
5334	38.75	37.78	106	120	24.7	217	39.39	37.50	0.3	-1.93	0.15	0.969
5371	38.76	38.28	264	183	37.8	243	40.28	38.00	0.3	-1.43	0.11	0.939
5457	36.71	36.60	978	26	5.4	62	39.03	35.40	0.2	-1.67	0.04	0.946
5474	37.18	37.36	165	29	6	36	39.82	37.26	0.3	-1.18	0.11	0.614
5850	38.82	37.59	155	138	25.5	220	39.26	37.30	0.3	-1.69	0.11	0.960
5921	38.36	37.80	274	122	25.2	153	39.28	37.50	0.2	-1.38	0.11	0.944
5964	38.48	37.79	111	120	24.7	220	39.67	37.50	0.3	-1.96	0.20	0.995
6140	38.34	37.00	127	90	18.6	126	39.29	37.38	0.3	-1.50	0.12	0.970
6384	38.69	39.75	148	129	18.6	230	40.79	39.48	0.2	-1.08	0.19	0.830
6946	37.11	36.65	1528	27	5.5	40	39.38	36.36	0.2	-1.44	0.03	0.974
7727	38.32	PQ	24	113	23.3	196	38.16	37.61	0.7	Too few H II regions		
7741	37.96	38.5	246	60	12.3	87	39.51	36.76	0.3	-1.35	0.06	0.823

Table 1. (Online only) General properties of the sample galaxies, H α images and resulting H II region catalogues. Calibration constant, in log of L (erg s $^{-1}$) per count in the H α image (col. 2), lower completeness limit of the LF (log L ; col. 3), number of H II regions catalogued (col. 4), image scale in pc per arcsec (col. 5), distance to the galaxy in Mpc (from Paper II; col. 6), and resolution (seeing, FWHM) in the H α image in pc (col. 7). N/A in col. 2 means no calibration available, in col. 3, PQ means poor quality LF and NDR means no disk H II regions. Cols. 8-9 tabulate the upper and lower limits (in log L) of the luminosity function; col. 10 the bin width used for the plotting and fitting of the LF, ranging from 0.2 to 0.7 dex as a function of the number of H II regions; col. 11 the value of the slope, a , of a single power law fitted to the data; col. 12 the combined error (in log L), including background effects and calibration errors, and col. 13 the coefficient of determination, r^2 , where values closer to unity indicate better fits.

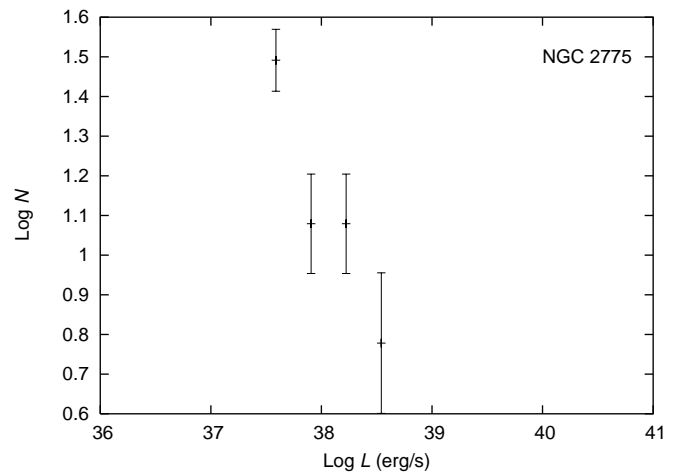
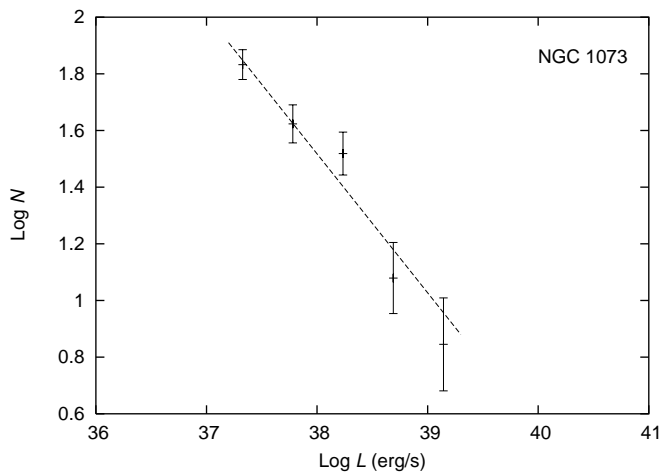
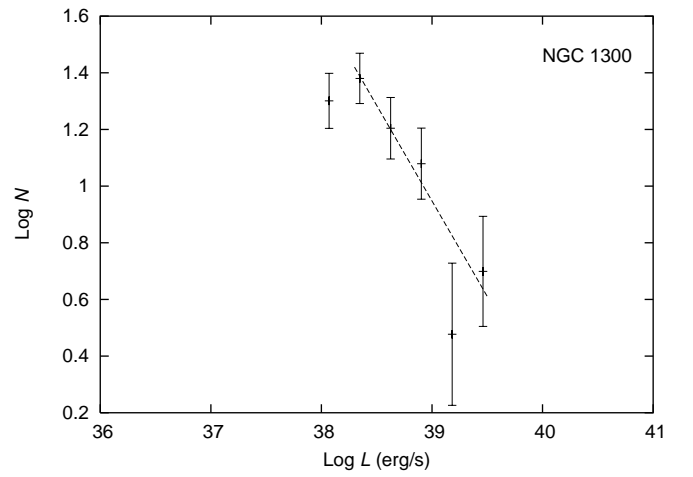
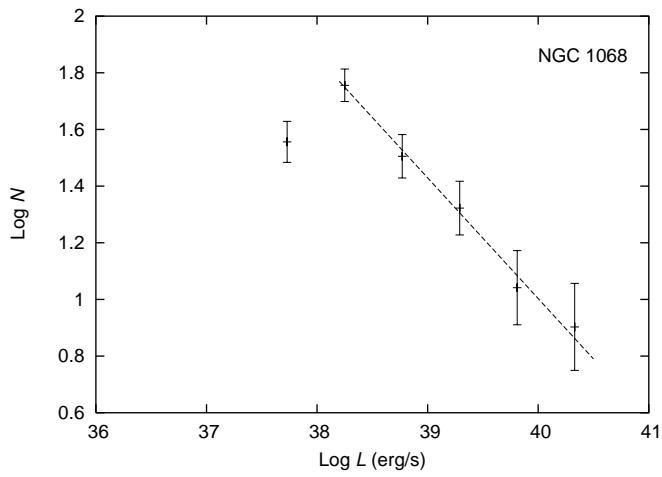
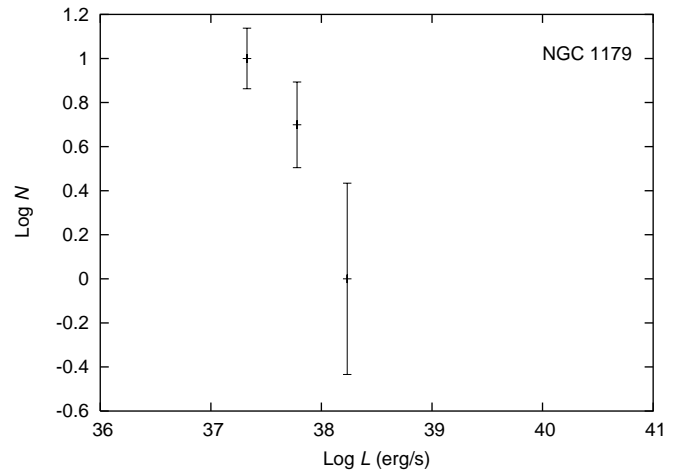
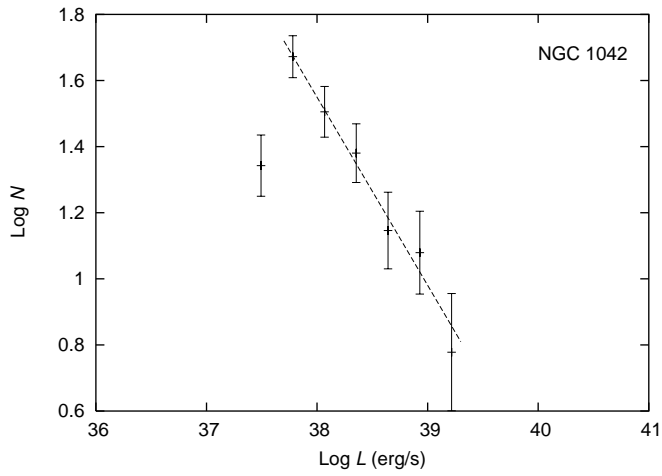
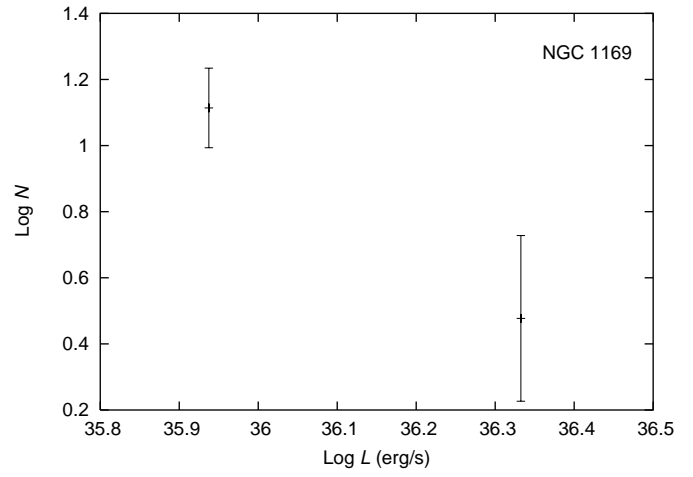
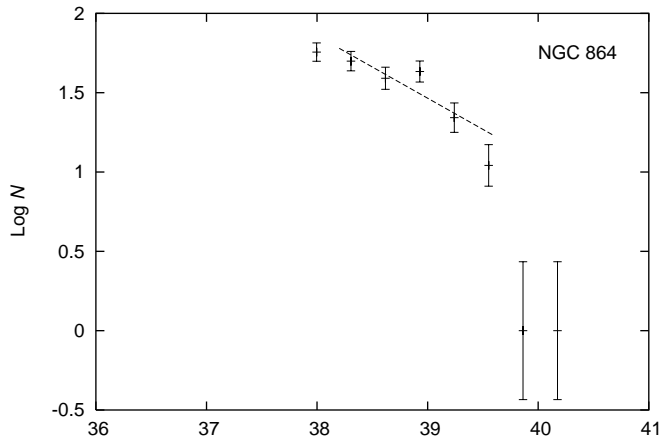


Fig. 1. (Continued)

Fig. 1. (Continued)

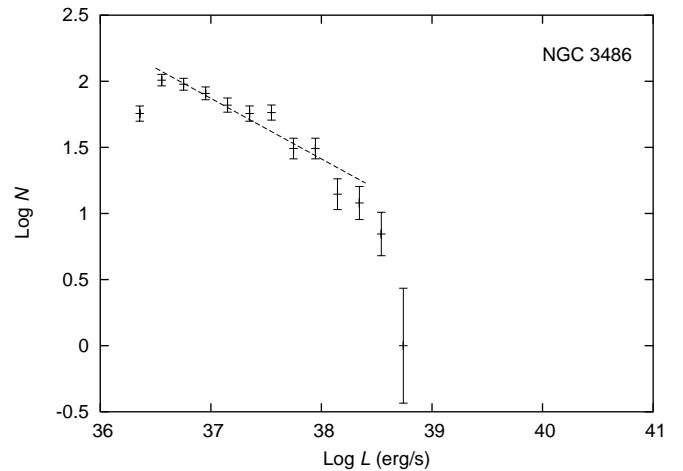
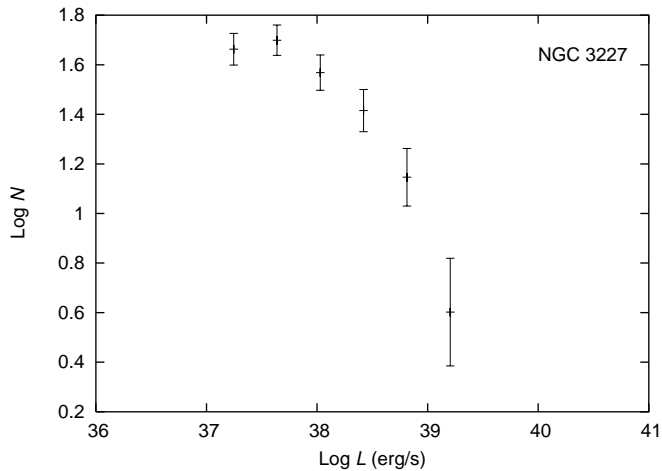
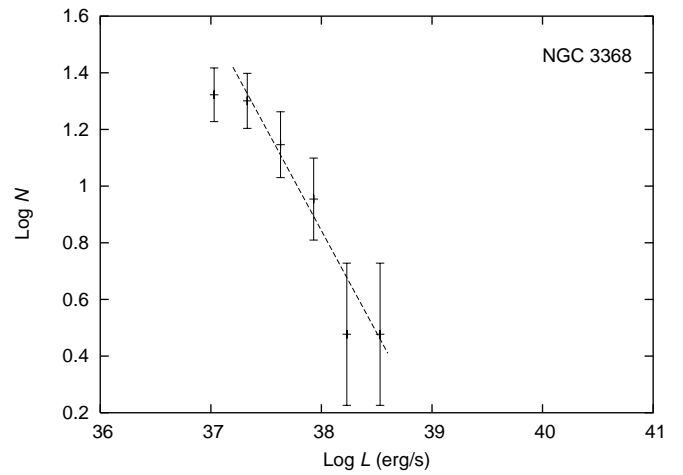
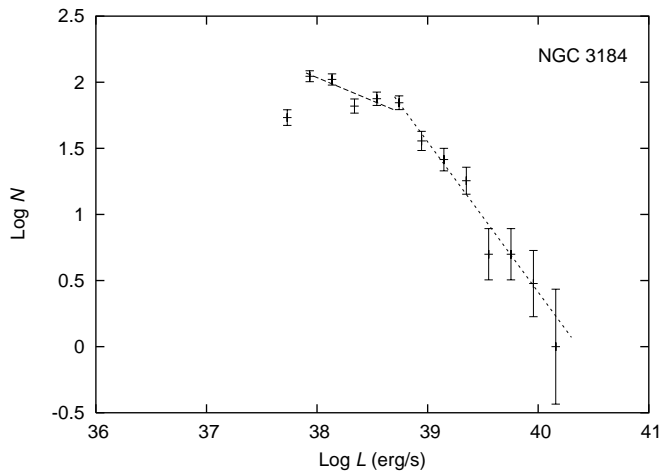
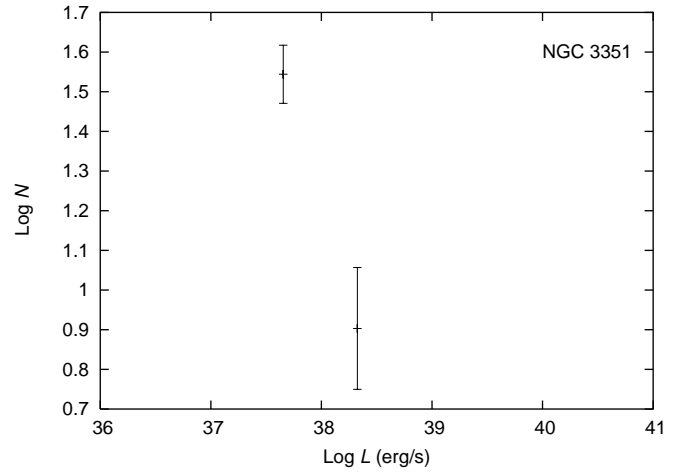
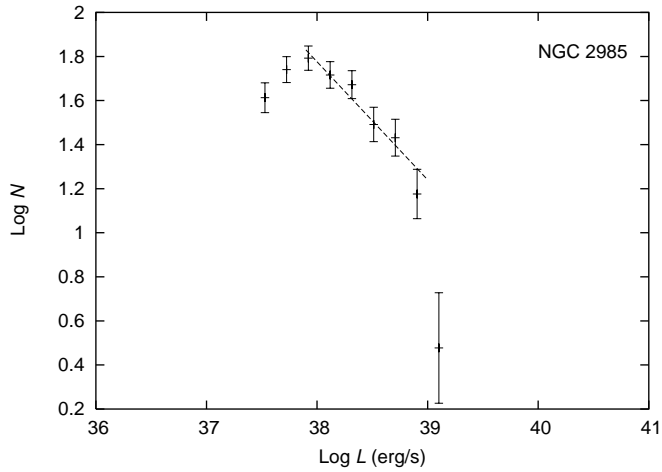
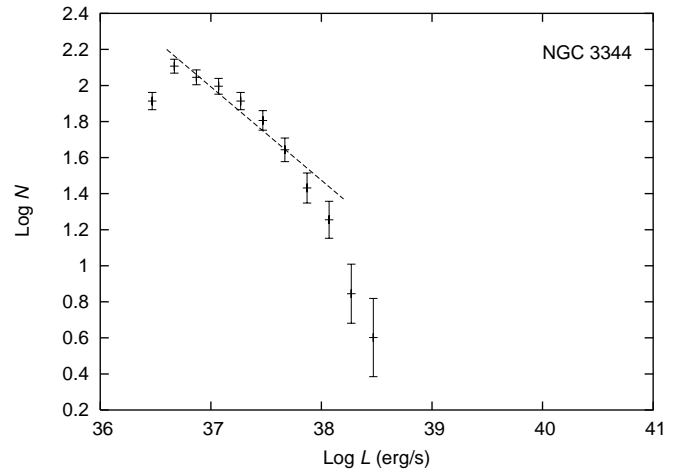
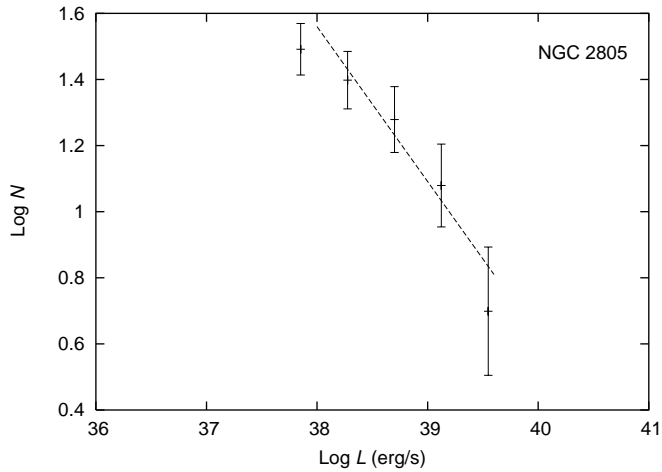


Fig. 1. (Continued)

Fig. 1. (Continued)

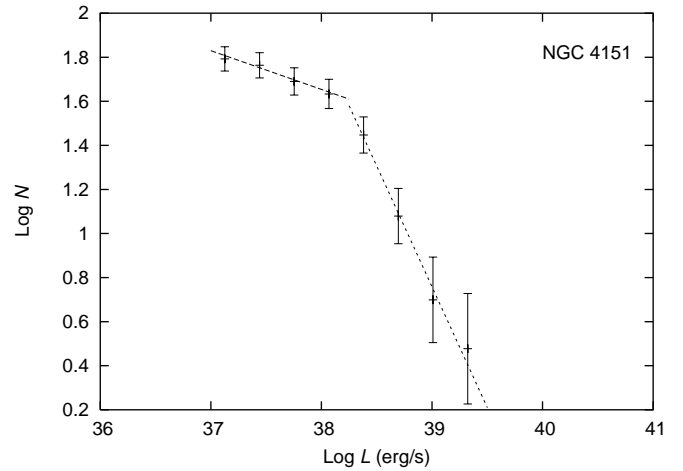
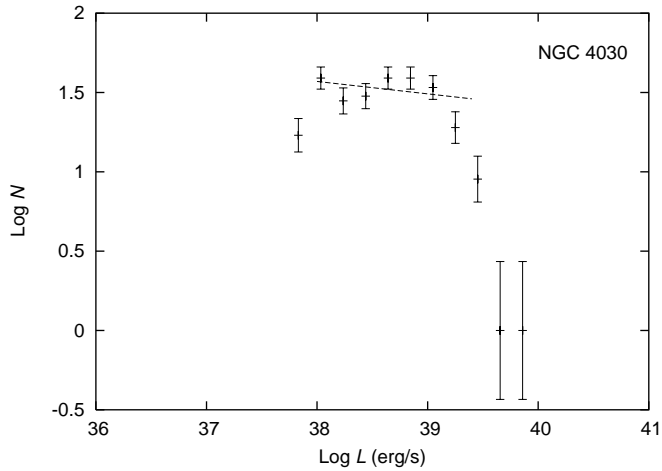
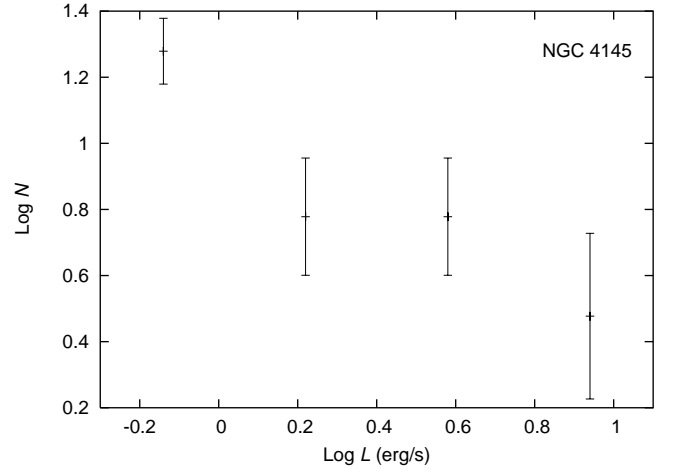
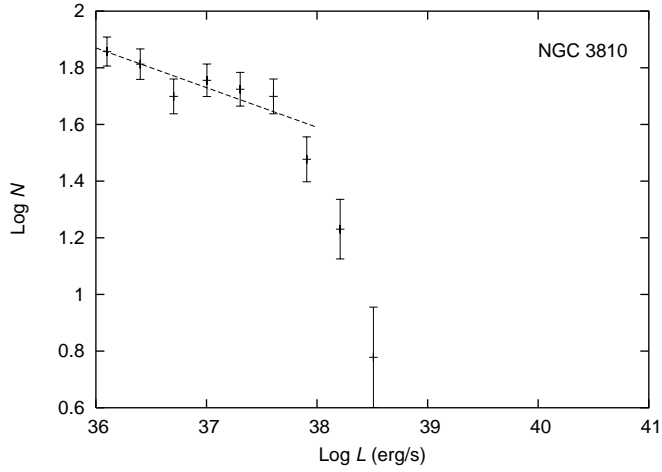
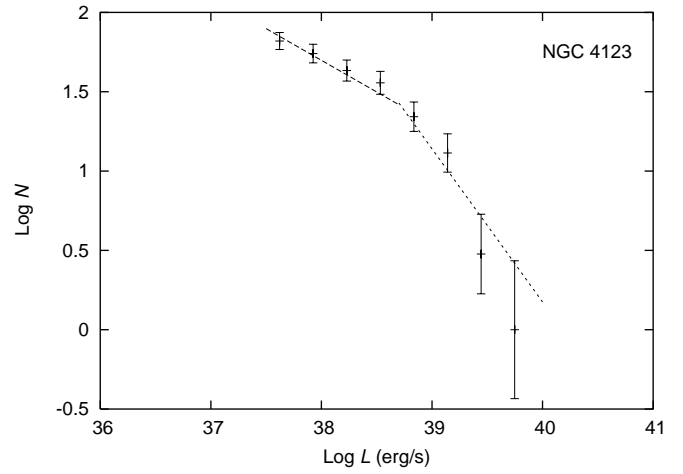
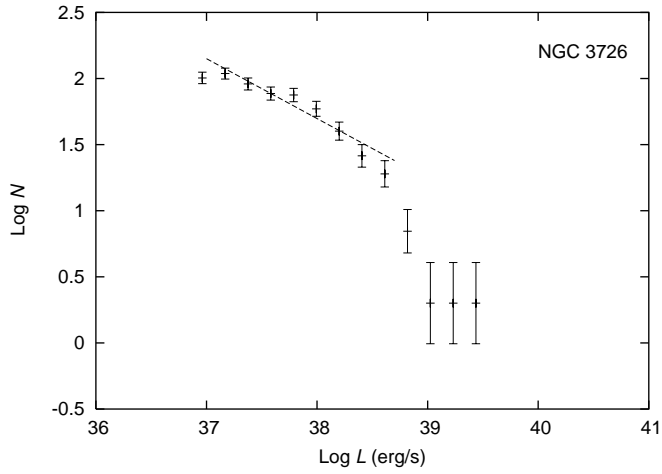
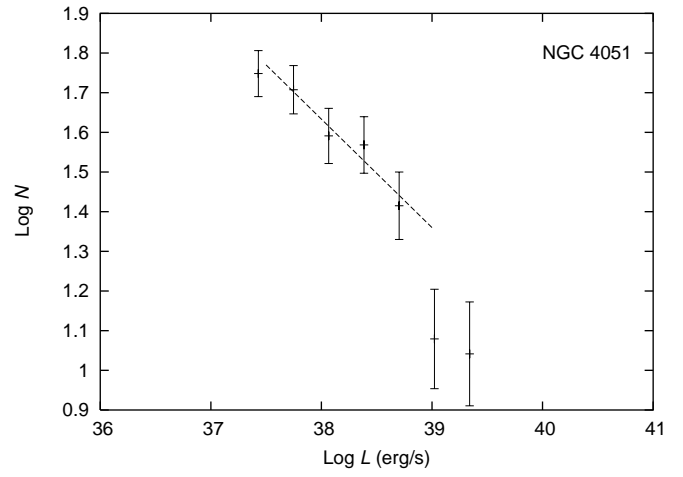
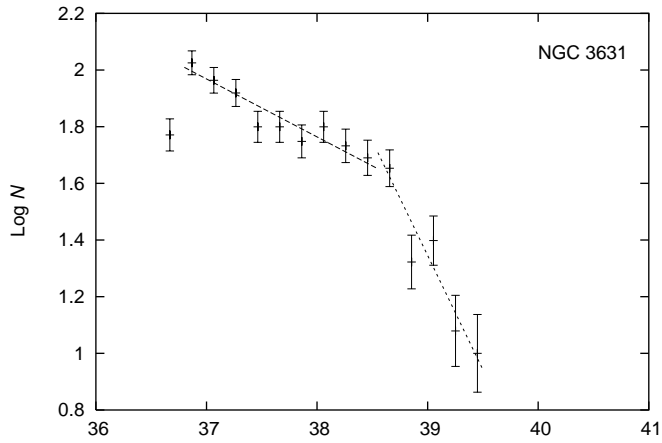


Fig. 1. (Continued)

Fig. 1. (Continued)

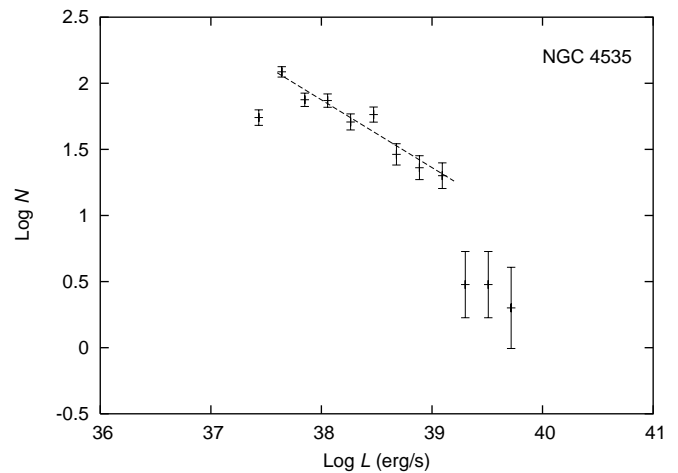
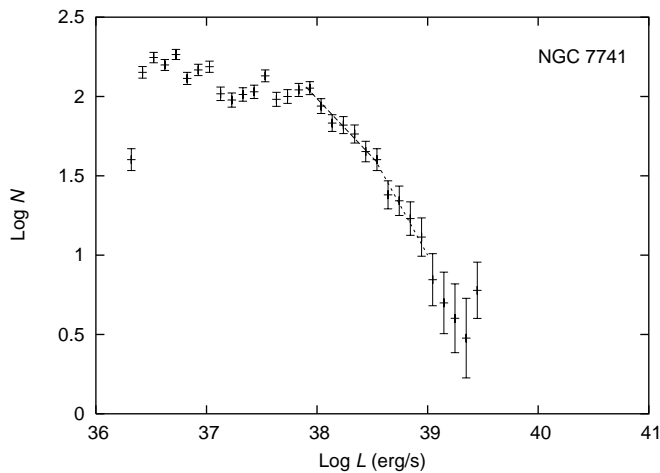
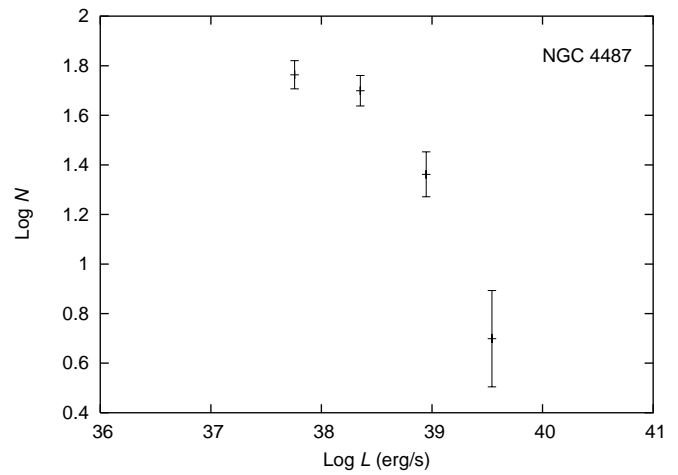
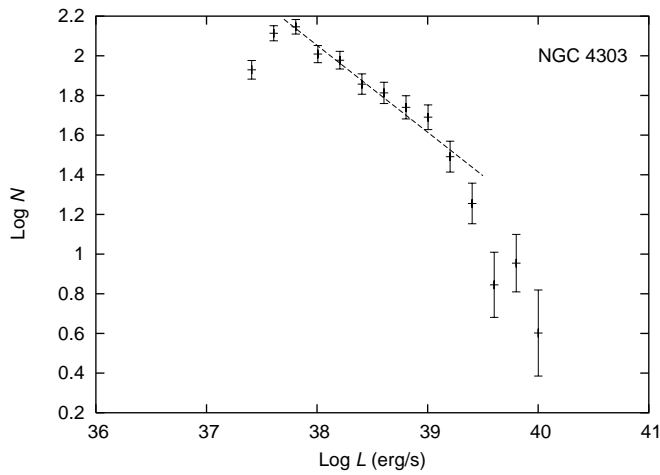
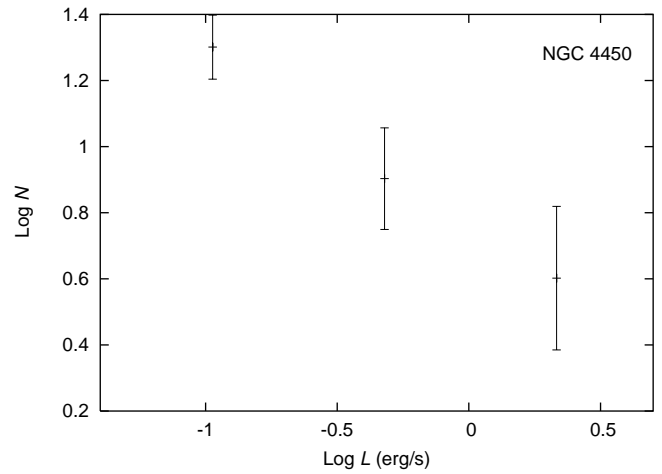
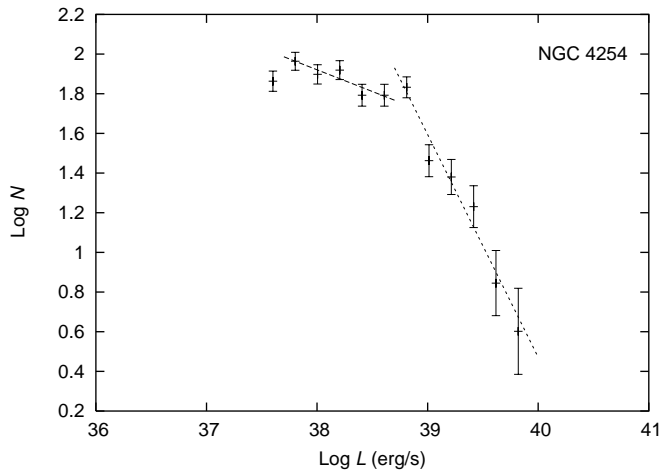
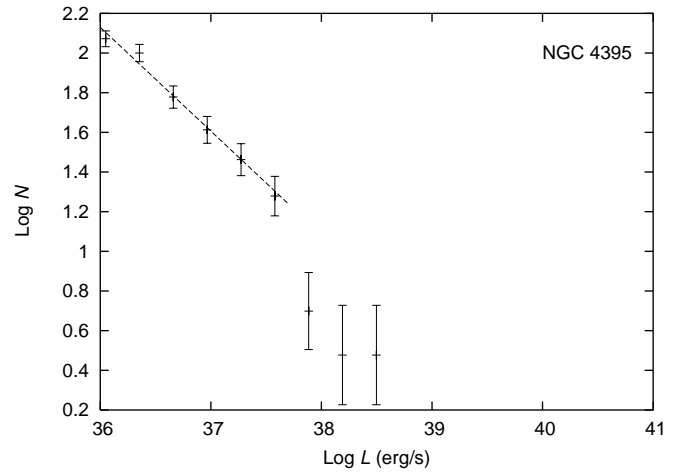
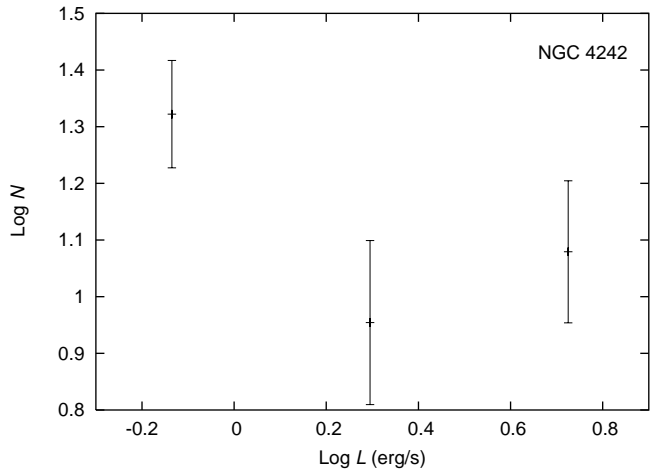


Fig. 1. (Continued)

Fig. 1. (Continued)

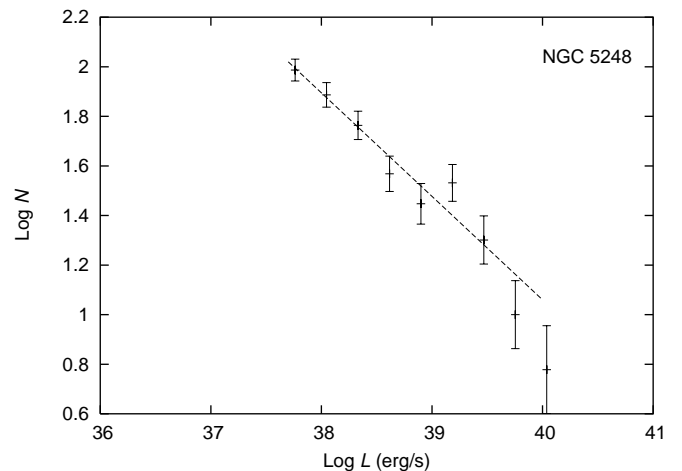
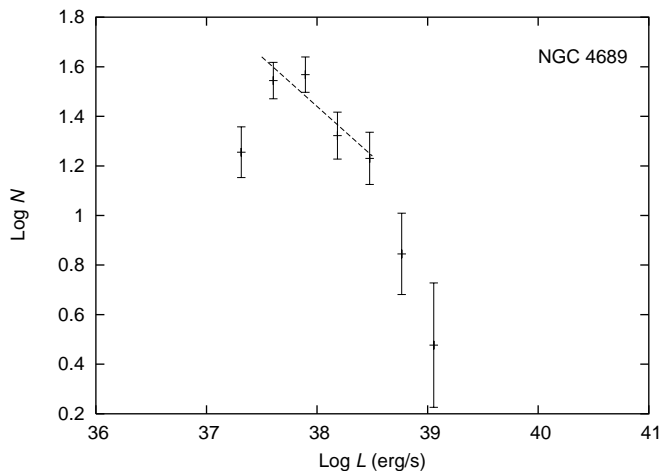
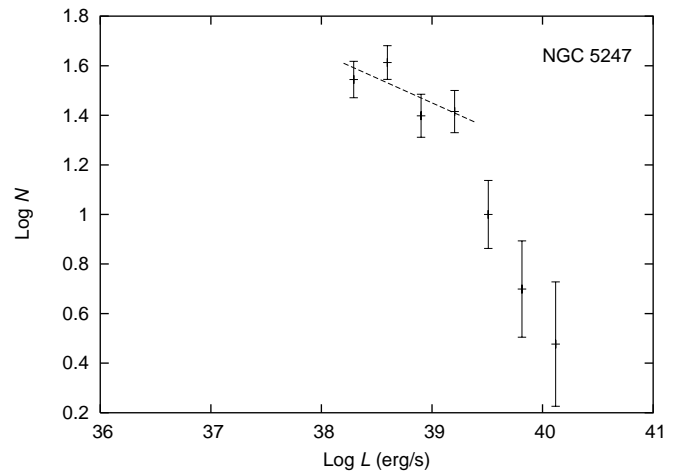
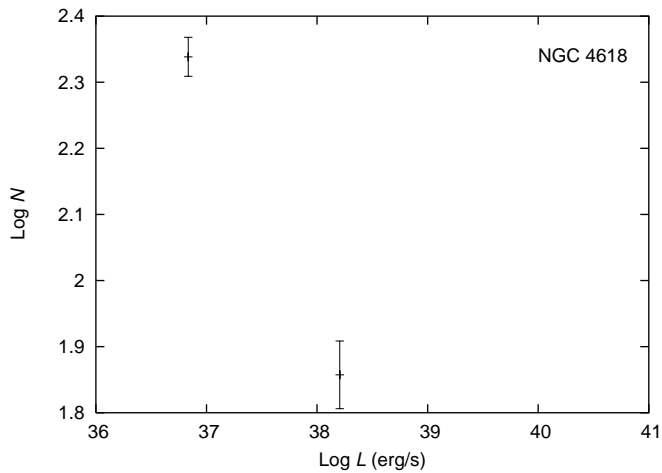
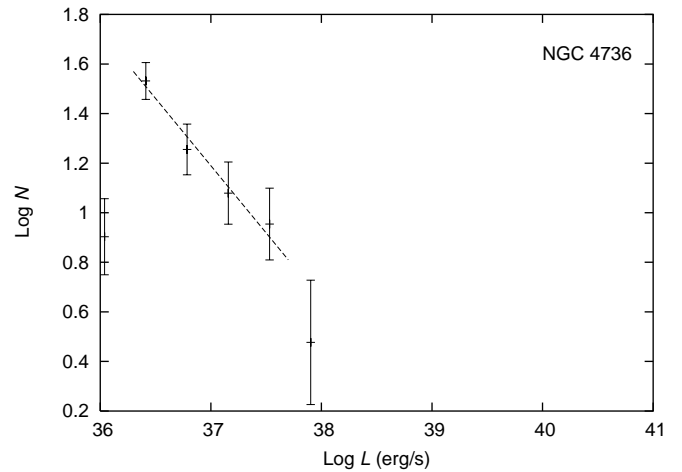
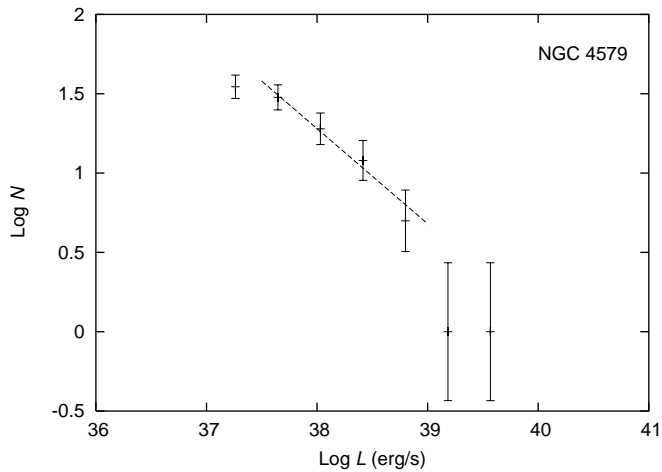
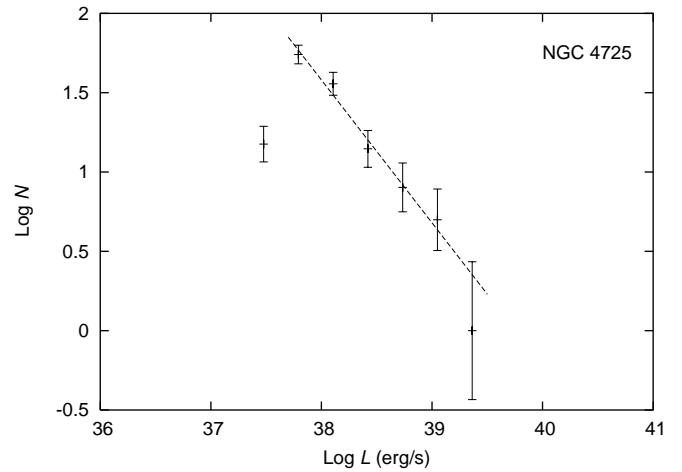
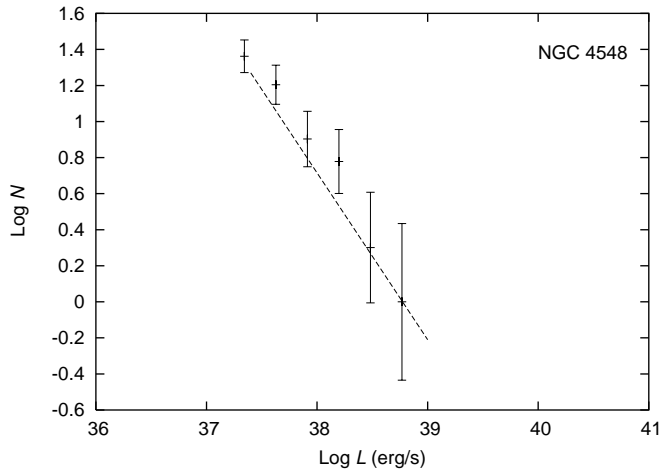


Fig. 1. (Continued)

Fig. 1. (Continued)

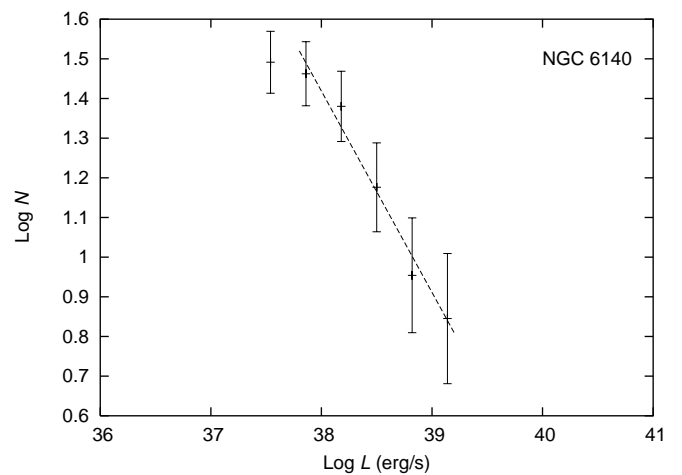
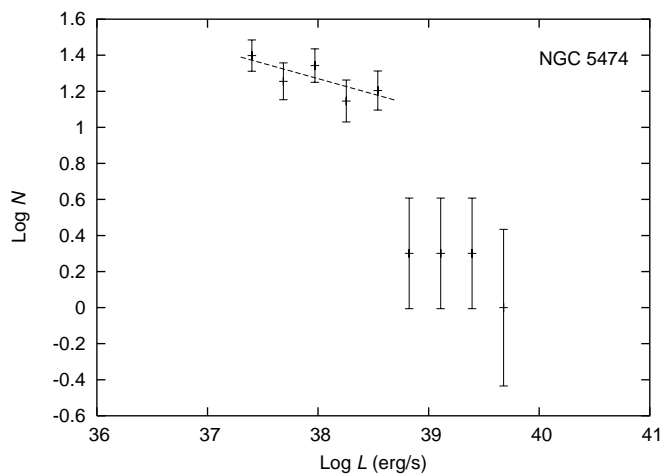
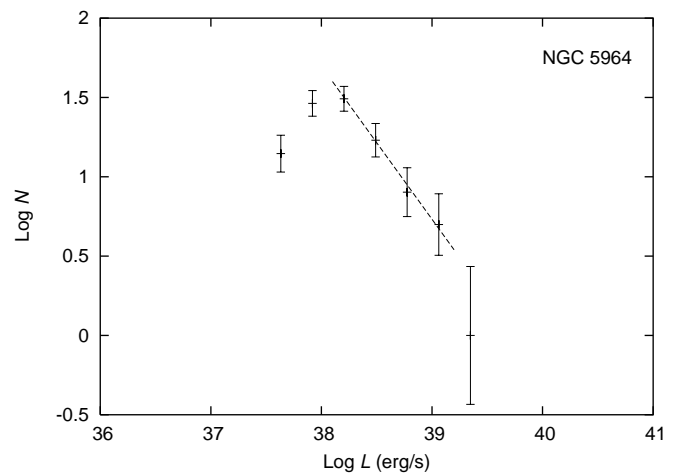
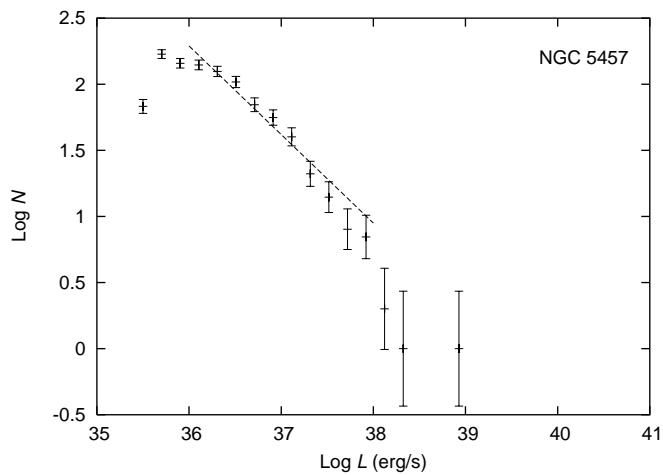
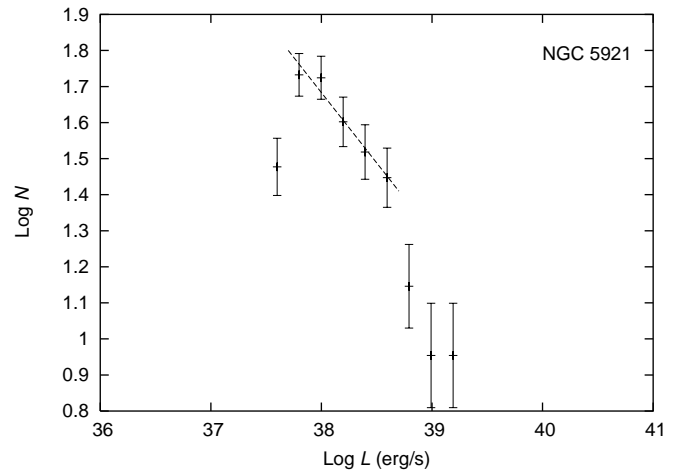
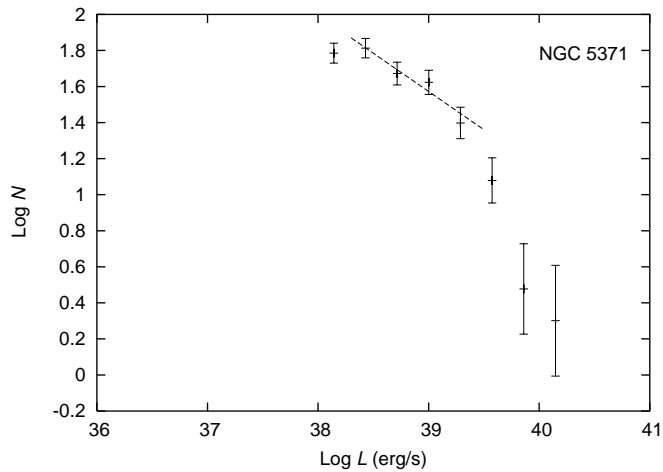
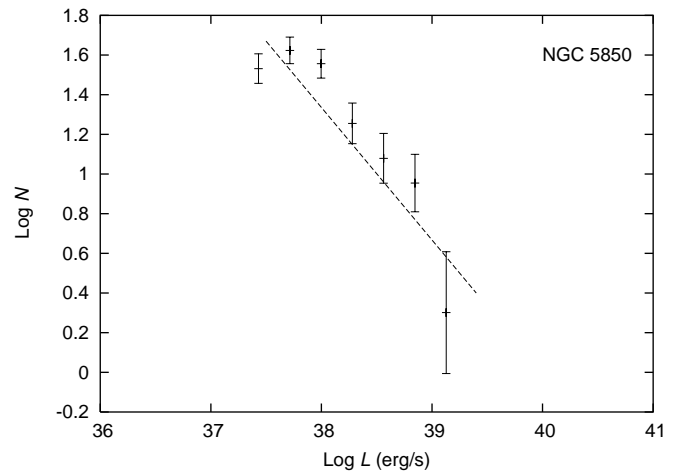
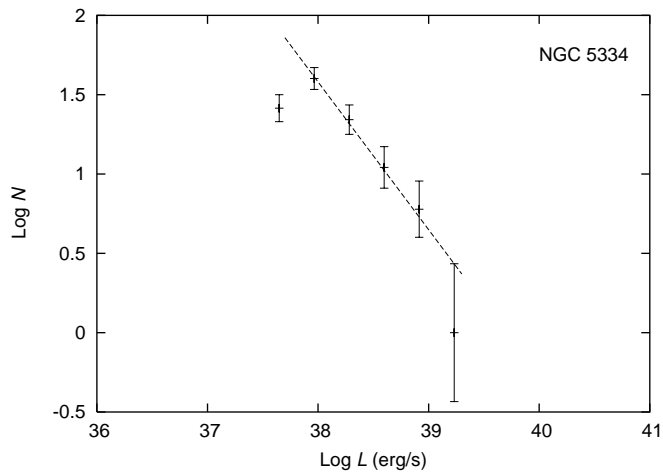


Fig. 1. (Continued)

Fig. 1. (Continued)

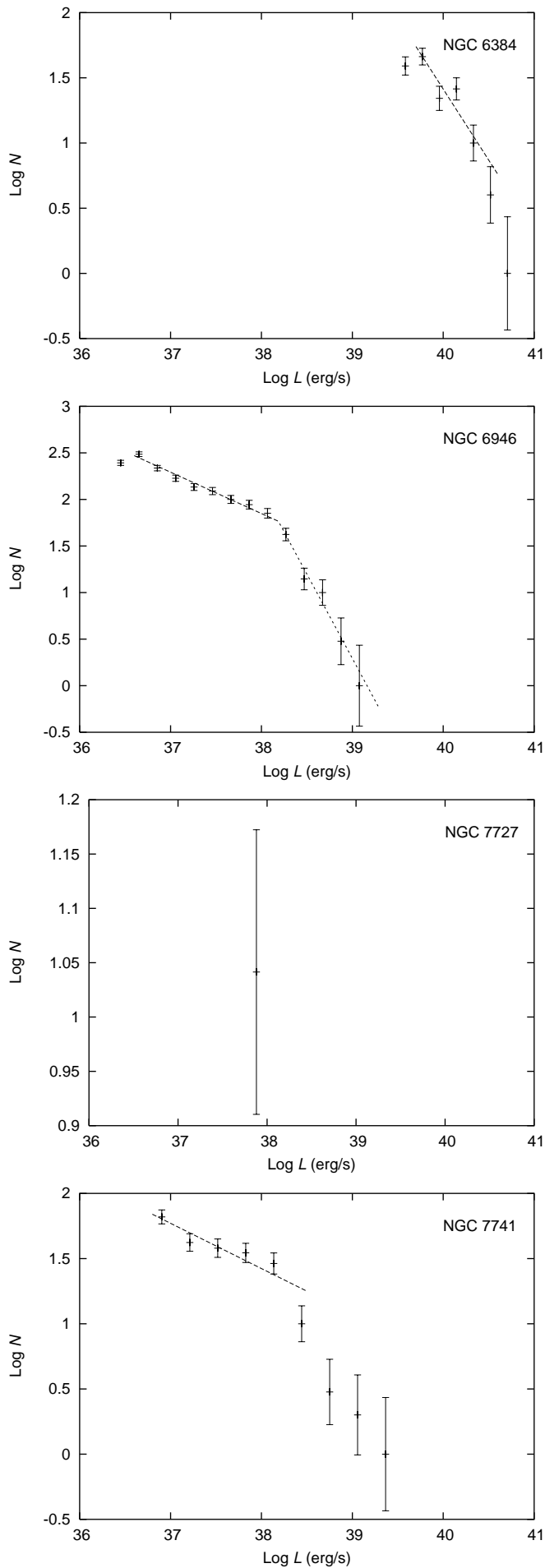


Fig. 1. (Continued)